is in good agreement with that calculated

$$\tau(\mathrm{PCL})/\tau_h(\mathrm{PPO}) = 0.9 \quad \text{(calculated)} \qquad (19)$$

The effect of chemical structure on the relaxation times is thus explained well by taking into account the moment of inertia of bond rotation in Kramers' rate constant at the low-friction limit.

Registry No. PPO (SRU), 25322-69-4; PEO (SRU), 25322-68-3.

References and Notes

(1) Stockmayer, W. H. *Pure Appl. Chem.* **1967**, *15*, 539.
(2) Rouse, P. E. *J. Chem. Phys.* **1953**, *21*, 1272.
(3) Zimm, B. H. *J. Chem. Phys.* **1956**, *24*, 269.
(4) Jones, A. A.; Brehm, G. A.; Stockmayer, W. H. *J. Polym. Sci., Polym. Symp.* **1974**, *No. 46*, 149.
(5) Bates, T. W.; Ivin, K. J.; Williams, G. *Trans. Faraday Soc.* **1967**, *63*, 1964.
(6) Matsuo, K.; Mansfield, M. L.; Stockmayer, W. H. *Macromolecules* **1982**, *15*, 935.
(7) Mashimo, S. *Macromolecules* **1976**, *9*, 91.
(8) Mashimo, S.; Chiba, A. *Polym. J.* **1973**, *5*, 41.
(9) Stockmayer, W. H.; Matsuo, K. *Macromolecules* **1972**, *5*, 766.
(10) Mashimo, S.; Nakamura, H.; Chiba, A. *J. Chem. Phys.* **1982**, *76*, 6342.
(11) Kramers, H. A. *Physica (Amsterdam)* **1940**, *7*, 284.
(12) Chandrasekhal, S. *Rev. Mod. Phys.* **1943**, *15*, 1.
(13) Mashimo, S.; Chiba, A.; Shinohara, K. *Polym. J.* **1974**, *6*, 170.
(14) Mashimo, S. *J. Chem. Phys.* **1977**, *67*, 2651.
(15) Mashimo, S.; Winsor, P.; Cole, R. H.; Matsuo, K.; Stockmayer, W. H. *Macromolecules* **1983**, *16*, 965.
(16) Davies, M.; Williams, G.; Loveluck, G. D. *Z. Elektrochem.* **1960**, *64*, 575.
(17) Nakamura, H.; Mashimo, S.; Wada, A. *Jpn. J. Appl. Phys.* **1982**, *21*, 1022.
(18) Iwasa, Y.; Chiba, A. *J. Polym. Sci., Polym. Phys. Ed.* **1977**, *15*, 881.
(19) Cole, R. H. *J. Phys. Chem.* **1975**, *79*, 1459, 1469.
(20) Cole, R. H.; Mashimo, S.; Winsor, P. *J. Phys. Chem.* **1980**, *84*, 786.
(21) Nakamura, H.; Mashimo, S.; Wada, A. *Jpn. J. Appl. Phys.* **1982**, *21*, 467.
(22) Baur, M. E.; Stockmayer, W. H. *J. Chem. Phys.* **1965**, *43*, 4319.
(23) Havriliak, S.; Negami, S. *J. Polym. Sci., Part C* **1966**, *14*, 99.
(24) Abe, A.; Hirano, T.; Tsuji, K.; Tsuruta, T. *Macromolecules* **1979**, *12*, 1100.
(25) Marchal, J.; Benoit, H. *J. Polym. Sci.* **1957**, *23*, 221.
(26) Scholtan, W.; Lie, S. Y. *Makromol. Chem.* **1964**, *81*, 14.
(27) Allen, G.; Booth, A. C.; Jones, M. M. *Polymer* **1964**, *5*, 195.
(28) Liao, T.-P.; Morawetz, H. *Macromolecules* **1980**, *13*, 1228.
(29) Volkenstein, M. V. "Configurational Statistics of Polymeric Chains"; Interscience: New York, 1963.
(30) Matsuo, K.; Stockmayer, W. H.; Mashimo, S. *Macromolecules* **1982**, *15*, 606.

Theory of Potentiometric Titration of Polyelectrolytes: A Discrete-Site Model for Hyaluronic Acid

Robert L. Cleland

Department of Chemistry, Dartmouth College, Hanover, New Hampshire 03755.
Received August 30, 1983

ABSTRACT: The potentiometric titration of weak polyacids which are fully ionized when completely neutralized is treated in terms of a conformation model of the tissue polysaccharide hyaluronic acid, for which the Manning parameter $\xi < 1$. The parameters of the model were chosen to fit approximately the unperturbed Kuhn length and its temperature coefficient. The part of the configurational free energy which depends on the degree of ionization α is the electrostatic free energy, where pair interactions are taken to be given by the simple Debye–Hückel screened Coulomb potential energy. The linear Ising model in the third-nearest-neighbor approximation is used to calculate the titration curve of $\Delta pK \equiv pK_a - pK_0$ as a function of α, where the apparent ionization constant K_a is defined by $pK_a \equiv pH + \log[(1-\alpha)/\alpha]$ and pK_0 is pK_a for $\alpha = 0$. The average excess free energy (referred to the uncharged state) is shown to be given, to a good approximation for the hyaluronate titration, by an extended Bragg–Williams (EBW) approximation. The resulting approximate titration curve is $\Delta pK/\alpha = (2/2.3kT)(u_1 + u_2 + ...)$, where u_p is the conformationally averaged excess free energy of interaction of a charged site with its pth nearest neighbor, to be summed over all neighbors. A rough numerical estimate of the sum was obtained from a rigid wormlike ("frozen worm") model for which the pair distances in the Debye–Hückel potential were taken as expansion-corrected unperturbed root-mean-square charge separations, as given by the conformational model. This estimate agreed approximately at several ionic strengths with that obtained from Monte Carlo calculations of the configurational partition function based on the same model. The latter estimate, corrected for the low dielectric constant of the polyion and for salt exclusion by use of a cylinder model, agrees reasonably well with experimental titration data for hyaluronate at low ionic strength I. The corrected result can be approximated at low I by the EBW result for the model of ionization sites spaced equally at distance b on a straight line: $\Delta pK/\alpha = (2\xi/2.3)\ln[1 - \exp(-\kappa b)]$, where κ is the Debye–Hückel screening parameter. The latter result approximates at low I that of the uniformly charged cylinder model with "radius" equal to the site spacing b, which is about 1.0 nm for hyaluronate.

This work concerns the potentiometric titration of the class of polyacids which, even when fully neutralized, are completely ionized (or nearly so) in the Debye–Hückel sense. According to the criterion of Manning,[1] complete ionization occurs for the infinite line charge model of polyelectrolytes when the charge density parameter ξ is less than unity, where ξ is defined by

$$\xi = e^2/DbkT \qquad (1)$$

In eq 1, e represents the electronic charge, D the bulk solvent dielectric constant, b the length per unit (electron) charge, k the Boltzmann constant, and T the absolute temperature. With the bulk dielectric constant D (=78.3) at 25 °C, $\xi = 0.716/b$ (b in nm), so that b must be greater than about 0.7 nm to meet this criterion. As b decreases below this distance, the Manning theory predicts increasing counterion condensation in the near vicinity of the polyion, which partly shields the polyion charge.

As a specific example the present work focuses on the polysaccharide hyaluronic acid, for which experimental titration data are available[2,3] at several values of the ionic strength I. Hyaluronate, the ionized form of the acid, for

0024-9297/84/2217-0634$01.50/0

which b = ca. 1.0 nm, is one of the few available polyions which meet the above criterion for complete ionization and which have a structure well enough defined to permit accurate estimates of charge spacing in terms of a conformational model.

The repeating unit in this linear polymer is an AB disaccharide: [D-glucuronic acid (A) (β-(1→3))-2-(acetylamino)-2-deoxy-D-glucose (B) (β-(1→4))]$_Z$, so that the polymer contains $2Z$ monosaccharides and Z ionizable groups located on the (A) glucopyranose rings of the ABAB... structure. The distance of separation of these groups will depend on the angles at the glycoside bonds (indicated above by β-(1→3) and β-(1→4)). Conformational calculations[4] suggest an average ionizable site separation of about 0.9–1.1 nm, depending on the energy parameters chosen to represent the molecule. Available experimental evidence supports the assumption, based on the Manning criterion, that hyaluronate is completely ionized in solution.[3]

The potentiometric titration data[3] were presented in the form of plots of pK_a against the degree of ionization α, where pK_a is defined, as in the case of acids of low molecular weight, by

$$pK_a \equiv pH + \log [(1 - \alpha)/\alpha] \quad (2)$$

The experimental data were compared to the results for pK_a obtained from theoretical treatments of the Poisson–Boltzmann equation for the infinite uniformly charged cylinder model of a polyion. The form of the data with respect to the variation of the ionic strength was fitted well by the result obtained from the analytical solution[5,6] for the surface potential of the cylinder from the linearized form of the equation and probably better by the numerical integration of the nonlinearized equation.[7] These fits require a choice of cylinder radius of about 1.0 nm, however, as well as neglect of specific terms in the electrostatic potential involving counterion size. This radius seems unreasonably large in view of estimates of 0.3–0.35 nm for the unhydrated radius from the partial specific volume[8] and small-angle X-ray scattering[9] or 0.55 nm for the shear radius from viscometry as interpreted by the wormlike chain model[10] to perhaps 0.7 nm for the salt-exclusion radius (to the counterion center for Na^+) from salt exclusion data.[8]

The uniformly charged cylinder is, at best, a crude approximation to an ionized polymer. A discrete-site model into which the conformational properties of the polyion can be incorporated has obvious advantages. In this work a discrete-site model is developed which essentially follows the approach to the electrostatic problem formulated long ago by Harris and Rice.[11] In addition, their use of the linear Ising model is also followed for statistical evaluation of the model but is carried here to the third-nearest-neighbor approximation. The results are found for the titration curve of the low-charge-density case to be reasonably approximated by an extension of the Bragg–Williams approximation familar from the theory of adsorption on linear chains. Numerical estimates are based on a conformational chain model.

Conformation Model

The chain model used in performing conformational calculations in this work has been described previously[12] in connection with a study of the unperturbed dimensions of hyaluronic acid. Briefly, this model consists of a sequence of the AB disaccharide repeating units mentioned above with an A terminal unit at the nonreducing chain end and a B terminal unit at the reducing end, the disaccharide units being numbered from 1 to Z. The substituted glucopyranose rings which constitute the monosaccharide residues are assumed to be rigid, so that interchain distances are determined by the coordinate geometry adopted for the monosaccharide units and the rotational angles about the glycoside bonds connecting them. When side-chain rotation is taken into account, the rotational angles about the bonds joining side chains to the rigid pyranose rings are also relevant variables.

The conformational (free) energy E for one specification of the bond angles may be written as follows:

$$E = E_1 + \sum_{j=2}^{Z-1} E_j + E_Z + \sum_{j=1}^{Z-1} E_{j,j+1} + \sum_{j=1}^{Z-2} E_{j,j+2} + \ldots \quad (3)$$

$$E_j = (E_{BA})_j + (E_B)_j + (E_A)_j + (E_{el})_j \qquad (j = 1, 2, \ldots, Z) \quad (4)$$

$$E_{j,j+1} = (E_{AB})_j + (E_{el})_{j,j+1} \qquad (j = 1, 2, \ldots, Z - 1) \quad (5)$$

$$E_{j,j+2} = (E_{el})_{j,j+2} \qquad (j = 1, 2, \ldots, Z - 2) \quad (6)$$

where the specific inclusion of E_1 and E_Z allows for possible end effects on the energy. As indicated in eq 4, the intrinsic disaccharide energy E_j includes conformational energy contributions which represent interactions within the individual monosaccharide units A_j and B_j, as well as the rotational potential energy $(E_{BA})_j$[12] for the rotation of the jth B unit about the C_1–O_g glycoside bond of the jth A unit (angle ϕ_{Aj}) and the C_3–O_g glycoside bond of the jth B unit (angle ψ_{Bj}), where O_g refers to the glycoside oxygen. Each of the terms $(E_A)_j$, $(E_B)_j$, and $(E_{BA})_j$ includes potential energies due to the usual short-range forces (van der Waals interatomic forces, dipole–dipole interactions, and bond rotation torsional forces). The $(E_{BA})_j$ can also contain the free energy terms contributed[12] by side-chain rotations (suitably averaged at a given ψ_{Bj} and ψ_{Aj} over the rotational angles about the bonds linking each side chain to the pyranose frame), but these turn out to play a relatively minor role in the conformational averages which determine the unperturbed dimensions, except for those which involve hydrogen bonding, when the latter is taken into account. For this reason, except where they were assumed to be involved in hydrogen bonding, side chains were fixed at their local energy minima as determined by calculation of the energy at 30° intervals of the side-chain rotation angles. Energies of a side chain involved in hydrogen bonding were averaged over similar rotation intervals to provide free energies at fixed ψ_{Bj} and ϕ_{Aj}. In this sense $(E_{BA})_j$ is a function only of ψ_{Bj}, ϕ_{Aj}, and T. The rotational potential energy $(E_{AB})_j$ is similar in nature to $(E_{BA})_j$ and represents contributions coming from the rotation of the $(j + 1)$th A unit about the C_1–O_g glycoside bond of the jth B unit (angle ϕ_{Bj}) and the C_4–O_g glycoside bond of the $(j + 1)$th A unit (angle ψ_{Aj}). As in the case of BA rotation, $(E_{AB})_j$ will be a function only a ψ_{Aj}, ϕ_{Bj}, and T.

The term $(E_{el})_j$ represents the electrostatic free energy due to the charging of the ionizable sites on the jth A unit (free energy of mobile ion atmosphere formation, ion–solvent or, more generally, ion–dipole interactions, etc.), while the term $(E_{el})_{j,j+1}$ represents the additional free energy introduced between j and $j + 1$ units by the charging of the ionizable sites on both units. The term $(E_{el})_{j,j+2}$ represents corresponding additional effects [above those contained in $(E_{el})_{j,j+1}$ and $(E_{el})_{j+1,j+2}$], due to second-neighbor ionization. Further terms can be formulated analogously.

The energy E is thus a function of all of the glycoside bond angles and T, so that thermodynamic properties which depend on conformational states must be obtained from partition functions. The assumption is reasonably made for β-linked polysaccharides (including cellulose and

its derivatives) that the potential energy terms from short-range forces can be neglected for second-neighbor monosaccharide units, such as A_j with A_{j+1}. In that case the partition function can be factored into a product of partition functions for each sequential disaccharide pair. For a disaccharide repeating unit, this means that only two partition functions need be evaluated when only short-range forces are considered. We choose the standard state to be the discharged polyacid, so that the product of these partition functions over the entire chain constitutes the standard-state partition function.

In carrying out conformational energy calculations for the disaccharide interactions, such as $(E_{BA})_j$ and $(E_{AB})_j$, the procedure used followed that in the previous work on conformation,[12] except that the example chosen for use here employed the coordinate geometry of Arnott and Scott,[13] which was used by Winter et al.[14] to describe the geometry of threefold helical sodium hyaluronate obtained by stretching thin films of the polymer under conditions of controlled humidity. The criterion for the choice of energy parameters of the present example was that the unperturbed dimensions should resemble those estimated from experiment[10] (Kuhn segment length, A_K = ca. 9.0 nm) and, in addition, that the experimental estimate[15] from viscosity data of the temperature coefficient of unperturbed dimensions (d ln A_K/dT = ca. −0.004 K^{-1}) should be reasonably accounted for. The example chosen gave A_K = 8.6 nm and d ln A_K/dT = −0.005 K^{-1} at 25 °C.

Calculations of unperturbed dimensions with various assumptions concerning the energy parameters[16] indicated that, in the context of the approximation of rigid pyranose rings, only those structural assumptions which invoked stiffening by hydrogen bonding or some other effect with a similar activation energy were capable of producing sufficiently large temperature coefficients. One such assumption, which sometimes had this effect, was use of a large anomer-effect correction (5–6 kcal mol^{-1}) to the threefold rotational energy potential about the glycoside bond suggested by work on rotations about C–O bonds in compounds containing substituted methoxyl groups.[17,18] Large negative temperature coefficients may also be due to internal flexibility within the pyranose rings, as assumed by Brant and Goebel,[19] who showed that values of d ln A_K/dT similar to the above resulted for appropriate energy parameters. The belief that hydrogen bonding may be an important factor in the conformational structure of hyaluronic acid is based on the postulate that breaking such bonds is responsible for the significant decrease in dimensions for hyaluronate in alkaline solution.[15,20]

Details of the calculation and the system of numbering the ring atoms may be found in the previous work.[12] A brief description of the assumptions made in the calculations for the illustrative example follows. Interactions between all pairs of nonbonded atoms were calculated from the Lennard-Jones potential energy function minimized at the sum of atomic radii corresponding to minimum interatomic contact distances in crystals (potential set 1′). Electrostatic dipole interactions, which make small contributions to the conformational energy, were included by assignment of partial charges to the atoms in order to simulate bond dipole moments; a value of 4 was chosen for the effective dielectric constant, but the actual value chosen has little effect on the results. The torsional bond potential about the glycoside C–O bonds was taken to be a symmetric threefold potential with a maximum value of 2.3 kcal mol^{-1}. Hydrogen-bonding energies were estimated from the potential energy function suggested by Momany et al.,[21] for which only the interatomic distances between the hydrogen-bonded atoms are required. As indicated in the previous work with a different method of estimating hydrogen bond energies, the only hydrogen bonds of conformational significance were those whose acceptors were the pyranose ring oxygens (O_5 of the A ring or O_5' of the B ring) from the hydroxyl groups attached to the carbon atoms (C_3 on A or C_4' on B) adjacent to glycosidic carbons of the succeeding pyranose unit along the chain. In these calculations the possible effects of solvent water on the hydrogen bond potential functions have been neglected, though such effects may be quite significant.

Electrostatic Free Energy

Thus far discussion of conformational energy contributions has been limited to those of the uncharged polyacid. The ionization of the uronic acid groups on the A rings will introduce additional energy contributions, designated by subscript "el" in eq 4–6. In this work only the charged site interactions with each other and with the mobile ions will be considered. Ion–dipole interactions with the solvent, as well as such interactions with the dipoles of the polyion, are undoubtedly important. Since similar effects occur in the case of the monomeric acid, however, these energies can be expected to appear in the free energy of ionization of the individual sites and will therefore contribute only to the $(E_{el})_j$ terms.

The partially ionized polyion represents a distribution of charges on or in organic material of relatively low dielectric constant D_0, which is immersed in a solvent of high dielectric constant D_1 composed of small mobile ions in water. Experiment has shown[22] that the effect of adding NaCl to water can be expressed by the equation $D_1 = D - 11C_3$, where C_3 is the molar concentration, so that the effect is a small one for the cases of interest.

Fixman[23] examined the validity of the Poisson–Boltzmann (PB) equation by functional expansion techniques and concluded that solutions to this equation, generalized to include non-Coulombic contributions to the mean potential, should be a good approximation for dilute polyelectrolyte solutions. Ideally, one would solve such an equation, at least in the usual Coulombic approximation, using the charge distribution as the source potential with the boundary conditions appropriate to the molecular geometry. The problem proves to be intractable except for models possessing simpler geometry than the wormlike chain, which would be appropriate for the present case. One such model is the infinite uniformly charged cylinder. The numerical results[7] of the solution of the PB equation for the latter model, when applied[3] to polyions of low ξ such as hyaluronate, indicate that only small corrections to the corresponding linearized (Debye–Hückel (DH)) equation are made by the more exact solution. Solutions of the DH equation for more suitable molecular models may therefore also be regarded as good approximations to solutions to the PB equation.

The approach in this section is, accordingly, to estimate the electrostatic energy of ionic interactions by adopting essentially the solution of Rice and Nagasawa.[24] These authors gave a solution to the DH equation for discrete sites located on a polyion chain which occupied a spherical region of dielectric constant different from D and which was permeated with the electrolyte solution in which the polyion was immersed. In the present work their solution will be modified with use of the simpler point of view taken with models having cylindrical symmetry that the dielectric constant appearing in the solution of the DH equation may be approximated by that of the bulk solvent. Corrections can then be discussed in terms of a polyion cylinder of low D_0 on which discrete sites are located.

The system of interest will be supposed to contain a single polyion having Z ionizable sites, of which a fraction $\alpha \equiv \zeta/Z$ are charged in a given state, so that the polyion consists of ζ charges and the accompanying ζ counterions. The polyion is immersed in bulk solvent of dielectric constant D (or D_1). All charged sites, as well as small ions in the system, will be taken to have unit (electron or proton) charge of magnitude e. The volume of the solution will be supposed large enough so that the polyion has no effect on the chemical potential of the salt component. In actual polyelectrolyte solutions, the constancy of this chemical potential can be assured, as in the Stigter–Hill solution model,[25] by considering the solution to be always at dialysis equilibrium with an electrolyte solution at concentration C_3^* of the salt component. The potentiometric titration data[3] for hyaluronic acid were reported on the latter basis. The Debye–Hückel screening parameter κ will be taken to be that of the added electrolyte, so that

$$\kappa = (4\pi e^2 n/DVkT)^{1/2} = 3.29(C_3^*)^{1/2}\ (\mathrm{nm}^{-1}) \qquad (7)$$

where n is the number of small mobile ions and the last equality refers to 25 °C and to C_3^* as a molar concentration, so that the ionic strength $I = C_3^*$.

Rice and Nagasawa[24] obtained the electrostatic free energy A_{el} of such a system by charging the small ions of the added electrolyte (free energy, A_{salt}), followed by charging the polyion with its counterions at constant κ (or C_3^*) with use of the solution they obtained to the DH equation. The result, with the above approximation and with omission of the exclusion effects of the polyion on small ions, may be written (their eq 7.1.23)

$$A_{el} = \frac{e^2}{D}\sum_{j=1}^{Z-1}\sum_{k>j}^{Z}\frac{\exp(-\nu_j\nu_k\kappa r_{jk})}{r_{jk}} + \sum_{j=1}^{Z}\nu_j(A_{el})_j + A_{salt} \qquad (8)$$

where the constants ν_j and ν_k will be set equal to one if site j (or k) is ionized and zero if not. In eq 8, the second term represents terms proportional to ζ, and hence α, which correspond to the $(E_{el})_j$ terms in eq 2. The terms $(E_{el})_{j,j+p}$ (p = 1, 2, ...), which correspond to the electrostatic interactions of the jth AB unit with its pth nearest neighbor, are seen to be given by simple screened Coulomb potentials. A similar result was reached by Schildkraut and Lifson.[26]

Since the polyion terms in eq 8 involve only the charge site separation r_{jk} as a variable for different conformational states at a given κ, the chain model is readily adapted to the estimation of the electrostatic energy, provided only that, as in the case of hyaluronic acid, the geometric location of these sites in the molecule is known. The assumption required in making this adaptation is that the average of eq 8 over all conformational states of each j, k pair is an adequate representation of the electrostatic free energy, an assumption which seems consistent with the basic statistical assumptions of the Debye–Hückel treatment.

The effect of introducing charges on nearest-neighbor sites (p = 1) in hyaluronate on the conformational energy of an ABA sequence can be estimated by computing the average potential energy of the short-range type with and without the added electrostatic potential energy of eq 8. The calculation merely involves averaging the potential energy for each state specified by the angle set $\phi_{Aj},\psi_{Bj},\phi_{Aj},\psi_{Bj}$ (at 15° intervals of each) in the usual fashion by weighting with the appropriate Boltzmann factor. The calculation of the average nearest-neighbor charge separation distance in hyaluronic acid from conformation models by the same averaging technique has been described previously.[4] The values obtained for the latter ranged from 0.9 nm in the fourfold helical structure[27] to 1.1 nm for a stiff hydrogen-bonded structure. For the conformational example of this work, the average charge spacing in 0.01 M salt is found to be 1.03 nm. The average value of $e^2\exp(-\kappa r_{j,j+1})/Dr_{j,j+1}kT$ is found to be 0.511 at 25 °C, which corresponds to the effective distance 1.00 nm in the screened Coulomb potential energy expressed as a single term. Inclusion of the electrostatic terms lowered the average short-range potential energy by 7 cal mol^{-1} ($0.012kT$), so that separation of the total conformational energy into independent short-range and electrostatic contributions would introduce only small error. The procedure used for higher neighbors is described in the section on numerical results.

Equation 8 as it stands refers only to one ionization state s specified by $[\nu_1, \nu_2, ..., \nu_Z]_s$, so that an averaging procedure is needed to give $\langle A_{el}\rangle$, the chain average of eq 8 over all states s, and the average $\alpha = \langle\nu_j\rangle$. This problem is taken up below in terms of the linear Ising model.

Free Energy of Ionization: Apparent pK

The electrostatic effects considered above will be assumed valid also when the polymer solution contains hydrogen ions. Since hyaluronic acid contains ionizable carboxylic acid groups, the free energy of ionization of such groups from the reference (undissociated) state of zero charge must be included in the total free energy. The chemical reaction may be written

$$\zeta(\text{–COOH}) = \zeta(\mathrm{H^+}) + \zeta(\mathrm{COO^-}) \qquad (9)$$

for which the free energy change ΔA_i of ionization may be written for a fractional degree of dissociation $\alpha = \zeta/Z$

$$(\partial\Delta A_i/\partial\alpha)_{T,\kappa,V} = Z(\mu_{H^+} + \mu^\circ_{COO^-} - \mu^\circ_{COOH}) \qquad (10)$$

where μ_{H^+}, $\mu^\circ_{COO^-}$, and μ°_{COOH} are the chemical potentials (per ion) of these species. The superscript zero suggests infinite dilution, since interactions of the COO^- ions with each other and with ions of the electrolyte are accounted for in eq 8 and interactions of the –COOH groups with other COO^- or COOH groups are neglected.

As usual the equilibrium constant K of eq 9 for single-site ionization is given as $-\ln K = (\mu^\circ_{H^+} + \mu^\circ_{COO^-} - \mu^\circ_{COOH})/kT$, so that eq 10 becomes

$$(\partial\Delta A_i/\partial\alpha) = 2.3ZkT(\mathrm{p}K - \mathrm{pH}) \qquad (11)$$

when the definitions of activity; $\ln a_{H^+} \equiv (\mu_{H^+} - \mu^\circ_{H^+})/kT$, $\mathrm{p}K \equiv -\ln K/2.3$, and $\mathrm{pH} \equiv -\ln a_{H^+}/2.3$, are substituted into eq 10. Similar free energy terms were included by Harris and Rice[11] for ionization of ion-pair complexes of COO^- groups with other univalent cations. Since, however, hyaluronate is assumed here to be completely ionized in the Debye–Hückel sense, such terms are neglected. The total free energy ΔA measured from the reference state of zero charge (free energy A_0) may then be written

$$\Delta A \equiv A - A_0 = \Delta A_i + \langle A_{el}\rangle + Z\alpha(A_{el})_j \qquad (12)$$

where the terms A_{salt} and the free energy of short-range potential energy terms have been absorbed in A_0 and the term in angular brackets is the ensemble average over the double sum in eq 8. The thermodynamic condition determining equilibrium at constant T, κ, and V is that ΔA be minimum with respect to the unconstrained variable α, so that minimization leads to

$$\frac{1}{kT}\left(\frac{\partial\Delta A}{\partial\alpha}\right) = 0 =$$

$$2.3Z(\mathrm{p}K - \mathrm{pH}) + \frac{Z}{kT}(A_{el})_j + \frac{1}{kT}\left(\frac{\partial\langle A_{el}\rangle}{\partial\alpha}\right) \qquad (13)$$

where eq 11 has been substituted. When eq 2 is introduced into eq 13 and the value of pK_a at $\alpha = 0$ is termed pK_0 and written $pK_0 \equiv pK + (A_{el})_j/2.3kT$, eq 13 becomes

$$\Delta pK \equiv pK_a - pK_0 = (\partial\langle A_{el}\rangle/\partial\alpha)/2.3ZkT + \log[(1-\alpha)/\alpha] \quad (14)$$

Linear Ising Model

In order to compute the titration curve of ΔpK as a function of α, the statistical average appearing in eq 14 over the various ionization states of the chain of Z sites must be evaluated. The averaging procedure is most satisfactorily handled by use of an appropriate form of the linear Ising model. As in the original application of this model to the case of magnetic dipoles,[28] the ionization case has two possible states $\nu_j = 0$ (not ionized) and $\nu_j = 1$ (ionized) at each of the Z sites, or 2^Z states in all. The chains in these various states each immersed in the same solvent constitute a grand canonical ensemble for which a grand partition function may be evaluated. A clear presentation of the theoretical basis of the general method has been given by Schwarz,[29] who applied the model to the cooperative binding of ligands (of which H^+ is an example) to a polymer chain in the nearest-neighbor ($p = 1$) approximation.[30] The results he obtained for the binding curve can be shown to be identical with those reported earlier by Harris and Rice[11] and by Hill,[31] who were interested in application to the potentiometric titration case. A more general formulation of the model to include higher neighbors has been given by Sasaki and Minakata,[32] who applied their results to the titration of poly(acrylic acid).

The probability that the polyion occurs in a given ionization state s specified by $[\nu_1, \nu_2, \ldots, \nu_Z]_s$ is proportional to $q_s = \exp(-A_s/kT)$, where A_s is the work of forming the state, here taken to be given by eq 8. The partition function Ξ, which is the sum of q_s over all 2^Z ionization states, may be conveniently expressed, as first shown by Kramers and Wannier,[33] as a matrix product in terms of a statistical weight matrix. The matrix may be formulated following the lucid presentation of Flory[34] for the analogous case of the rotational isomer chain model. The statistical weight matrix $\mathbf{W}$ will be taken to have as its elements, in the nearest-neighbor case, the statistical weight $w_{\tau\upsilon}$. The ionization states (τ) for chain element j index the rows and those (υ) for element $j+1$ index the columns of $\mathbf{W}$. For the nearest-neighbor case, elements j are single AB units, so that $\tau = 0$ and 1 represent the possibilities for ν_j, and $\upsilon = 0$ and 1 those for ν_{j+1}. The ionization free energy $u_0 \equiv \mu^\circ_{COO^-} - \mu^\circ_{COOH}$ may be assigned to any state for which $\nu_{j+1} = 1$ and the free energy $u_1 \equiv (A_{el})_{j,j+1}$ (when $k = j+1$ in eq 8) to disaccharide unit $j+1$, when both $\nu_j = 1$ and $\nu_{j+1} = 1$, so that the matrix $\mathbf{W}$ may be written

$$\mathbf{W} = \begin{array}{c} \\ (0) \\ (1) \end{array} \begin{array}{c} \begin{array}{cc} (0) & (1) \end{array} \\ \begin{bmatrix} 1 & \upsilon \\ 1 & \upsilon\upsilon_1 \end{bmatrix} \end{array} \quad (15)$$

where $\upsilon \equiv \exp(-u_0/kT)$ and $\upsilon_1 \equiv \exp(-u_1/kT)$. The assumption that the value of υ for the chain terminal units may be different from that for the internal units requires the assignment of the values υ' and υ'' to υ for the left- and right-hand terminal units, respectively. The statistical weight matrices corresponding to these units can be found by assuming a nonionized unit beyond the left-hand terminal unit:

$$\mathbf{W}_1 = \begin{bmatrix} 1 & \upsilon' \\ 0 & 0 \end{bmatrix} \qquad \mathbf{W}_Z = \begin{bmatrix} 1 & \upsilon'' \\ 1 & \upsilon''\upsilon_1 \end{bmatrix}$$

The partition function is then extracted[34] by writing

$$\Xi = \mathbf{U}\mathbf{W}_1\mathbf{W}^{Z-2}\mathbf{W}_Z\mathbf{U}^T \quad (16)$$

where $\mathbf{U} = [1\ 1]$ and superscript T indicates the transpose. Since the first row of $\mathbf{W}_1$ is the same as that of $\mathbf{W}$ when the assumption is made that $\upsilon' = \upsilon'' = \upsilon$, eq 16 may be simplified[34] to

$$\Xi = \mathbf{U}'\mathbf{W}^Z\mathbf{U}^T \quad (17)$$

where $\mathbf{U}' = [1\ 0]$. Inclusion of the free energy u_0 of the isolated ionized units in the chain configurational energy gives Ξ the character of a grand partition function, since it contains an energy term for every conceivable ionization state of the Z chain units. The value of Ξ is given in terms of the eigenvalues λ_0 and λ_1 of $\mathbf{W}$ by[29]

$$\Xi = \left(\frac{1-\lambda_1}{\lambda_0-\lambda_1}\right)\lambda_0^{Z+1} - \left(\frac{1-\lambda_0}{\lambda_0-\lambda_1}\right)\lambda_1^{Z+1} \quad (18)$$

where λ_0 and λ_1 are the larger and smaller eigenvalues, respectively, which are readily obtained by solving the characteristic equation to give

$$\lambda_0 = \{(\upsilon\upsilon_1 + 1) + [(\upsilon\upsilon_1 - 1)^2 + 4\upsilon]^{1/2}\}/2 \quad (19)$$

and λ_1 differs by having a negative sign before the radical. For large enough Z, the quantity λ_1^{Z+1} in eq 18 can be ignored, so that

$$\Xi = \lambda_0^{Z+1}\left(\frac{1-\lambda_1}{\lambda_0-\lambda_1}\right) \quad (20)$$

which is identical with the result of previous nearest-neighbor treatments of this problem.[11,30,31]

An alternative procedure for evaluating Ξ, as suggested by Flory,[34] is merely to carry out the multiplication of eq 17 numerically, most simply on the digital computer by successive squaring of the matrix $\mathbf{W}$. The values of Ξ obtained in this way are identical with those from eq 20 even for relatively small Z, provided λ_0 and λ_1 are sufficiently different.

In order to include the second-neighbor terms in Ξ, the maneuver often suggested[30,34] is to write the matrix $\mathbf{W}$ for successive pairs of ionization sites, so that the states of j and $j+1$ are indexed by τ and those for $j+1$ and $j+2$ by υ. The overlap represented by including the states of $j+1$ in both rows and columns requires that the matrix element $w_{\tau\upsilon}$ be set to zero when the state of $j+1$ in a row is different from that in the column, since this represents a nonexistent state. As in the nearest-neighbor case, only free energy terms assignable to the $j+2$ unit [i.e., u_0, $u_1 = (E_{el})_{j+1,j+2}$, and $u_2 = (E_{el})_{j,j+2}$] will appear in the matrix for $j+2$, and then only [as υ or $\upsilon_i \equiv \exp(-u_i/kT)$] when $\nu_{j+2} = 1$; otherwise the matrix element is unity (for zero energy contribution). Thus, the matrix may be written ($k = j+2$)

$$\mathbf{W}_k = \begin{array}{c} \\ (00) \\ (10) \\ (01) \\ (11) \end{array} \begin{array}{c} \begin{array}{cccc} (00) & (10) & (01) & (11) \end{array} \\ \begin{bmatrix} 1 & 0 & \upsilon & 0 \\ 1 & 0 & \upsilon\upsilon_2{}^* & 0 \\ 0 & 1 & 0 & \upsilon\upsilon_1 \\ 0 & 1 & 0 & \upsilon\upsilon_1\upsilon_2 \end{bmatrix} \end{array}$$

$$(k = 3, 4, \ldots, Z+1) \quad (21)$$

The quantity $\upsilon_2{}^*$ is written for the 101 sequence to indicate that the average second-neighbor interaction will, in general, be different from that in the 111 sequence. With the same assumptions used in the nearest-neighbor case, the matrix for $j+2 = 2$ may be written

$$\mathbf{W}_2 = \begin{bmatrix} 1 & 0 & 0 & 0 \\ 0 & \upsilon' & 0 & 0 \\ 0 & 0 & \upsilon & 0 \\ 0 & 0 & 0 & \upsilon'\upsilon\upsilon_1 \end{bmatrix}$$

$\mathbf{W}_Z$ will be the same as $\mathbf{W}_k$ with υ'' in place of υ. The

partition function then reads

$$\Xi = \mathbf{U}\mathbf{W}_2\mathbf{W}_k^{Z-3}\mathbf{W}_Z\mathbf{U}^T \tag{22}$$

Again, following Flory, $\mathbf{W}_2$ can be replaced by $\mathbf{W}_2'$ with elements $(1, v', v, v'vv_1)$ in the first row and $\mathbf{U} = [1\ 1\ 1\ 1]$ by $\mathbf{U}' = [1\ 0\ 0\ 0]$. The first row of $\mathbf{W}_2'$ is now identical with that of $\mathbf{W}_k^2$ and eq 22 becomes identical with eq 17 when we again assume $v' = v'' = v$.

The evaluation of Ξ can, in principle, still be carried out by solving for the largest eigenvalue of $\mathbf{W}_k$. The algebra is involved, however, since the roots (or at least the first root) of a fourth-degree polynomial must be obtained. A discussion of the solution by a recursive method has been given by Marchi and Vila.[35] The alternative method used above involving the successive numerical squaring of the matrix is computationally simpler, when the numerical value of Ξ may be obtained from eq 17.

Higher neighbor interactions in eq 3 (or eq 8) can be handled in analogous fashion by using successively larger matrices $\mathbf{W}_k$, a $2^p \times 2^p$ matrix being required to include up to pth-neighbor interactions. The matrix is constructed, as before, to account for the new unit added in the v index, with a factor v_i $(i = p - f)$ (or v_i^*, etc.; see above) occurring in the matrix element each time ν_{j+f} and ν_{j+p} $(f = 0, 1, \ldots, p - 1)$ are both unity and a factor v occurring where ν_k $(k = j + p)$ is unity. The partition function will be given by eq 17 in each case, and the matrices are not given in detail.

Standard relations of statistical thermodynamics may be used to evaluate ensemble-average thermodynamic functions from the partition function Ξ. The average degree of ionization α and the free energy $\langle A_{el}\rangle$, which are needed to calculate ΔpK from eq 14, as well as the average energy $\langle E_{el}\rangle$ and entropy $\langle S_{el}\rangle$, related by $\langle A_{el}\rangle = \langle E_{el}\rangle - T\langle S_{el}\rangle$, will be of interest. The relationships needed have been given in a convenient form by Harris and Rice (cf. eq 21, 22, and 27 of ref 11a), which are quoted with appropriate change of notation:

$$\alpha = \frac{1}{Z}\left(\frac{\partial \ln \Xi}{\partial \ln v}\right)_T = \left(\frac{\partial \ln \lambda_0}{\partial \ln v}\right)_T \tag{23}$$

$$\langle A_{el}\rangle/ZkT = -\ln \Xi/Z + \alpha \ln v \tag{24}$$

$$\langle S_{el}\rangle/Zk = -\frac{1}{Zk}\left(\frac{\partial\langle A_{el}\rangle}{\partial T}\right)_\alpha = \ln \Xi/Z + \frac{1}{Z}\left(\frac{\partial \ln \Xi}{\partial \ln T}\right)_v - \alpha \ln v = -\langle A_{el}\rangle/ZkT + \frac{1}{Z}\left(\frac{\partial \ln \Xi}{\partial \ln T}\right)_v \tag{25}$$

The derivative of $\langle A_{el}\rangle/ZkT$ needed in eq 14 and that of $\langle S_{el}\rangle/ZkT$ may be readily obtained by differentiation with respect to α and use of the relation

$$\left(\frac{\partial \ln \Xi}{\partial \alpha}\right)_T = \left(\frac{\partial \ln \Xi}{\partial \ln v}\right)_T\left(\frac{\partial \ln v}{\partial \alpha}\right)_T = Z\alpha\left(\frac{\partial \ln v}{\partial \alpha}\right)_T \tag{26}$$

where eq 23 has been used. The results are

$$\frac{1}{ZkT}\left(\frac{\partial\langle A_{el}\rangle}{\partial \alpha}\right)_T = \ln v \tag{27}$$

$$\frac{1}{Zk}\left(\frac{\partial\langle S_{el}\rangle}{\partial \alpha}\right)_T = \frac{1}{Z}\left[\frac{\partial}{\partial \alpha}\left(\frac{\partial \ln \Xi}{\partial \ln T}\right)_v\right]_T - \ln v \tag{28}$$

Substitution of eq 27 into eq 14 then leads to

$$\Delta pK = \log\left[\frac{v(1-\alpha)}{\alpha}\right] \tag{29}$$

Table I
Calculated Results for Titration of Hyaluronic Acid at $I = 0.01$; Third-Neighbor Approximation

α	$\langle S_{el}\rangle/Zk$[a] Ising	S_m/Zk[b] random	ΔpK[c] Ising	ΔpK[c] BW
0.0528	0.206	0.206	0.032	0.037
0.101	0.326	0.327	0.063	0.072
0.204	0.503	0.506	0.134	0.146
0.303	0.608	0.613	0.207	0.217
0.404	0.667	0.674	0.283	0.289
0.509	0.685	0.693	0.365	0.365
0.596	0.667	0.674	0.432	0.428
0.708	0.598	0.604	0.518	0.508
0.797	0.501	0.505	0.582	0.571
0.908	0.306	0.307	0.659	0.651

[a] Calculated from eq 25 with the following energy parameters: $u_1/kT = 0.514$; $u_2/kT = 0.201$; $u_3/kT = 0.110$. [b] Calculated from eq 30. [c] Calculated from eq 29 with the same parameters as in a; for the Bragg-Williams approximation (BW): $\Delta pK = 2(0.825)\alpha/2.3 = 0.717\alpha$.

Comparison of eq 29, eq 2, and the first equality of eq 14 confirms that $v = K_0/a_{H^+}$.

Numerical Results

Ising Model. The calculation of the partition function Ξ by matrix squaring as a function of v, Z, and T is straightforward once values of the average electrostatic energy for the various neighbor pairs have been chosen. Values of α were then obtained by carrying out the differentiation indicated in the first equality of eq 23 with use of the numerical method of Rutledge.[36] Evaluation of ΔpK at each value of v followed immediately from eq 29. The entropy of mixing charged and uncharged sites was computed, when desired, from eq 25 by carrying out an additional numerical differentiation with respect to temperature. In performing the latter operation, the u_p (including u_0) were taken independent of T in order to avoid including entropic contributions due to interaction with the solvent (from temperature dependence of κ and D) and from hydrogen bonding. This procedure also ensures that the energy $\langle E_{el}\rangle$ computed from the temperature derivative of Ξ is identical with the ensemble-averaged energy.

In the nearest-neighbor case when Z was taken to be 1024, values of α calculated from eq 23 were found to be within 0.001 of the exact result for infinite Z:[30] $\alpha = (\lambda_0 - 1)/(\lambda_0 - \lambda_1)$, for nearest-neighbor electrostatic energies (up to 0.5 kcal mol^{-1}) typical of hyaluronic acid. The matrix-squaring procedure was then applied with this value of Z to cases involving neighbors of higher order.

The results of the calculation of $\langle S_{el}\rangle$ from eq 25 for the third-neighbor approximation with the illustratitive example in 0.01 M salt are compared in Table I with S_m, the entropy for random mixing of charged and uncharged sites, given by

$$S_m = -kZ[(1-\alpha)\ln(1-\alpha) + \alpha \ln \alpha] \tag{30}$$

The differences are seen to be at most about 1% in the 0.01 M case and they increase to at most about 2% in the 0.001 M case.

Extended Bragg-Williams Approximation. The above result suggests that a useful approximate form of eq 14 might be obtained by substitution for $(\partial\langle A_{el}\rangle/\partial\alpha)$ of $[\partial(\langle E_{el}\rangle - T\langle S_{el}\rangle)/\partial\alpha)_T$ to give

$$\Delta pK = \frac{1}{2.3ZkT}\left(\frac{\partial E_{el}}{\partial \alpha}\right)_T - \frac{1}{2.3Zk}\left[\left(\frac{\partial S_{el}}{\partial \alpha}\right) - \frac{\partial S_m}{\partial \alpha}\right]_T \tag{31}$$

where the final term in eq 14 has been replaced by the

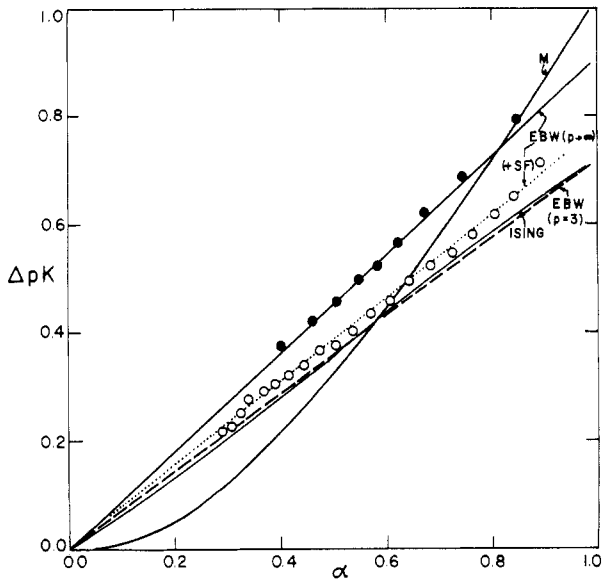

Figure 1. Theoretical titration curves for hyaluronic acid at salt concentration C_3^* = 0.01 M as calculated for the illustrative example by matrix squaring (Ising model) for three nearest neighbors. For comparison the corresponding extended Bragg–Williams (EBW) model is shown for p = 3 nearest neighbors and for many-neighbor convergence ($p = \infty$) in the frozen worm approximation as described in the text (see also Figure 2). The dotted line shows the effect on the EBW curve ($p = \infty$) of the Skolnick–Fixman (SF) corrections made as described in the text. The curve labeled M gives the result calculated for hyaluronic acid (ξ = 0.7) from the discrete-site theory of Manning for $\xi < 1$ (eq 63 of ref 49). The points represent experimental data for hyaluronic acid at C_3^* = 0.01 M reported previously ((○) ref 3; (●) calculated[3] from the data of Laurent[2]).

derivative of eq 30. A common assumption in potentiometric titration theories is that the entropy term in brackets in eq 31 can be neglected. This approximation suggests use of the corresponding random approximation to $\langle E_{el} \rangle$

$$\langle E_{el} \rangle = \alpha^2[(Z-1)u_1 + (Z-2)u_2 + ... + u_{Z-1}] \quad (32)$$

Equation 32 represents an extension to many neighbors of the approximation to the average ensemble energy suggested 50 years ago by Bragg and Williams[37] and will be termed here an "extended Bragg–Williams approximation" (EBW). Substitution of eq 32 into eq 31 for large Z leads to

$$\Delta pK = 2\alpha(u_1 + u_2 + ...)/2.3kT \quad (33)$$

in complete analogy to the result for the nearest-neighbor case given by Hill[31] in the Bragg–Williams approximation.

The titration data for the illustrative example calculated from eq 23 and 29 (again for I = 0.01) are compared in Table I with the result of eq 33, which is $\Delta pK = 0.717\alpha$ for the values chosen for u_p/kT (to p = 3) based on the "frozen worm" model to be described below. The values of the u_p have been assumed throughout this work to be given by the completely ionized chain, with neglect of the small variations which can be expected due to the occurrence of nonionized states in a given sequence of neighbors; i.e., v_j is assumed equal to v_j^*, etc. The values of ΔpK from the Ising model (eq 29) differ from those of eq 33 by a maximum of about 0.012 pK unit, as illustrated by the comparative plot of the two equations in Figure 1. For I = 0.001 the deviations are somewhat larger, up to a maximum of about 0.02 pK unit. The deviations increase very little in going from the second- to the third-neighbor approximation.

Further neighbors can therefore be expected to cause the average slope of the two plots to increase together without affecting the relative agreement. Since the matrix calculations become increasingly lengthy as larger matrices are introduced, the effects of further neighbors were approximated in terms of eq 32 or 33.

It may be worth mentioning that the demonstration concerning the close agreement of $\langle S_{el} \rangle$ and S_m in the case discussed above is not essential to the argument concerning the agreement of the EBW approximation and the Ising model with respect to the titration curve. Assumptions concerning the separate contributions of $\langle E_{el} \rangle$ and $\langle S_{el} \rangle$ to $\langle A_{el} \rangle$ do not affect the calculated titration curve. The use of the EBW approximation (eq 32) therefore remains valid in any case, *provided* the assumption of random entropy of mixing is retained.

Statistical Model. For the completely ionized chain the sum in eq 32 is just the excess free energy A_c (referred to the uncharged chain) associated with the configurational partition function Q_Z

$$Q_Z = \sum_{\omega} \exp(-E_\omega/kT) \quad (34)$$

summed over all conformational states ω. The quantity E_ω for a given conformation is, in principle, the potential of mean force obtained by averaging over the positions of all solvent molecules. Here, E_ω has been assumed to be given by eq 3 with omission of the irrelevant terms $(E_A)_j$, $(E_B)_j$, and $(E_{el})_j$, which do not contribute to the interaction energy between monosaccharide units. The chain consists of Z (=p + 1) disaccharide units with unit A_i fixed in position and orientation at the origin and therefore has p + 1 BA and p AB rotations. The rotation of unit B_Z about unit A_Z contributes to Q_Z a factor q_{BA}, the BA rotation partition function, which has no effect on the electrostatic energy. Since the u_p are by definition, free energies, the appropriate relation is

$$A_c(Z) = [(Z-1)u_1 + (Z-2)u_2 + ... + u_p] = -kT \ln (Q_Z/Q_{Z0}) = -kT \ln (Q_p/Q_{10}{}^p) \quad (35)$$

where $Q_{Z0} = Q_{10}{}^p q_{BA}$ is the corresponding function for the uncharged chain, $Q_p \equiv Q_Z/q_{BA}$, and $Q_{10} \equiv q_{AB}q_{BA}$ is the disaccharide unit partition function. The factorization indicates the independence of the rotational energies $(E_{AB})_j$ and $(E_{BA})_j$ for the uncharged chain. The resulting free energy $A_c(Z)$ will then include appropriately weighted contributions from the electrostatic interactions and the configurational entropy changes resulting from the effects of these interactions on conformational alternatives.

The (free) energies E_1, $E_{1,2}$, ..., E_p, $E_{p,p+1}$ are included in the partition function Q_p, along with all higher neighbor electrostatic interactions. The probability P_j that the glycoside angles associated with $(E_{BA})_j$ and $(E_{AB})_j$ in the uncharged chain are in a given angular state is given by

$$P_j(\phi_{Aj},\psi_{Bj},\phi_{Bj},\psi_{Aj}) = \exp[-(E_{AB})_j/kT] \exp[-(E_{BA})_j/kT]/Q_{10} \quad (36)$$

The ratio in the last equality of eq 35 may be written in terms of the P_j

$$Q_p/Q_{10}{}^p = \sum_{\omega} \left(\prod_{j=1}^{p} P_j\right) \exp(-E_{el}/kT) \quad (37)$$

where E_{el} is taken to represent the first term in eq 8 for a given conformation.

Since there are 576 states for each AB or BA set for angular intervals of 15°, direct summation of eq 36 rapidly becomes unwieldy even with suppression of angle pairs of relatively high energy. Evaluation of Q_1/Q_{10} for the case p = 1 with the present conformational example at I = 0.01 gave $A_c(2)/kT$ = 0.521, of which 0.511, as given above, is contributed by the average electrostatic energy. For p =

2, drastic limitations on the angle sets included are required to perform the direct sum. However, Monte Carlo methods can be invoked by assigning probabilities P_j in eq 36 from the potential energy scheme and using appropriate ranges of random numbers for each state to choose the angle pairs. The electrostatic term in eq 36 may then be evaluated by specifying the coordinates of the ionized sites according to a given sequence of randomly chosen angle pairs for each glycoside rotation and performing the double sum in eq 8 with all $\nu_j = 1$. By appropriate suppression of ionization at some sites (one or more $\nu_j = 0$), chain sequences involving nonionized states corresponding to the matrix elements υ_i^* can also be handled. In this way chains of up to 50 or more disaccharide units can readily be generated for use in estimating the partition function, as discussed in the second following section.

"Frozen Worm" Model. As a first approximation, a much simpler expedient was employed. Introduction of the assumption $u_p = e^2 \exp(-\kappa r_p)/r_p D$ into eq 33 gives

$$\Delta pK = (2\alpha/2.3)(e^2/DkT)\sum_p \exp(-\kappa r_p)/r_p = e\psi_j/2.3kT \quad (38)$$

where r_p represents the effective distance to the pth nearest neighbor which gives the correct average value $\langle \exp(-\kappa r_{j,j+p})/r_{j,j+p} \rangle$ from the conformation model. This assumption essentially ignores the entropic contributions to $A_c(Z)$, which will be seen to be relatively small. The second equality of eq 38 is the well-known result first derived by Overbeek,[38] in terms of the average electrostatic potential ψ_j at site j.

The distance r_p used in eq 38 for $p = 1$ was 1.00 nm, as discussed above. In the present approximation r_p was approximated for higher neighbors by the unperturbed root-mean-square end-to-end distance for a chain of p units, which will be similar to the corresponding ionizable site distance. The series of terms obtained in this way converged in eq 38 for $I \geq 0.02$ within a contour length $L = A_K$ (where the unperturbed Kuhn length A_K corresponds to Z = ca. 9 disaccharide lengths for this example[10]). The question of the dependence of A_K on ionic strength is discussed below; for the present model such dependence was neglected. As the ionic strength decreased below 0.02, convergence required more terms.

When L increases above A_K, the effect of expansion due to intramolecular excluded volume effects on the values of r_p becomes significant. Yamakawa and Stockmayer[39] treated the problem of the excluded volume for a wormlike chain and computed the theoretical expansion factor α_R in a single-contact approximation as a function of the dimensionless chain contour length L/A_K

$$\alpha_R^2 \equiv \langle R_e^2 \rangle_Z / \langle R_e^2 \rangle_{Z0} = 1 + K(L/A_K)z + \ldots \quad (39)$$

where $\langle R_e^2 \rangle_Z$ is the mean-square end-to-end distance in a good solvent for a chain of Z units, z is the usual excluded-volume parameter defined by

$$z \equiv (3\pi/2)^{3/2} B L^{1/2}/A_K^{1/2} \quad (40)$$

where B is a constant for a given polymer–solvent pair, and $K(L/A_K)$ is a function which increases from nearly zero at $L = A_K$ to the coil limiting value $^4/_3$ for infinite L/A_K.

An estimate of the average r_p can be made provided one assumes that the chain length dependence in $K(L/A_K)$ and z predicted theoretically on the basis of short-range forces is also obeyed for the long-range electrostatic forces. This kind of behavior has been assumed previously[9] for hyaluronate in terms of the Orofino–Flory treatment[40] of the expansion factor; the results expressed as unperturbed viscosities and dimensions calculated from data at $I = 0.2$ resembled those calculated from data for the uncharged polymer in acid solution. The procedure therefore seems reasonable, at least for high ionic strengths.

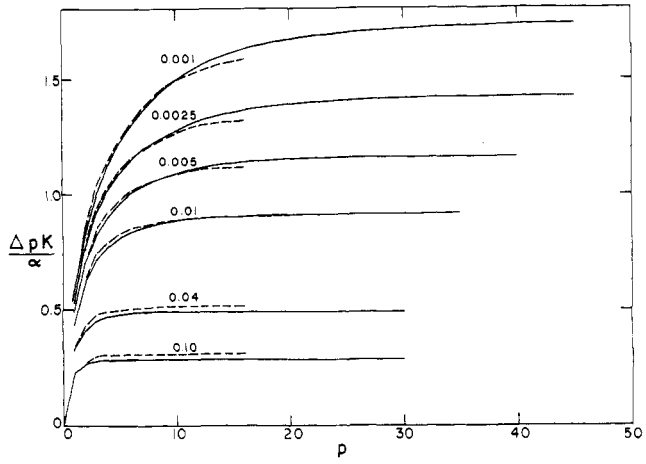

Figure 2. Contributions to $\Delta pK/\alpha$ (see eq 33) from the p nearest neighbors in the extended Bragg–Williams approximation. The solid lines show results for the illustrative conformation model in the frozen worm approximation to the sum. The dashed lines present the results from the Monte Carlo estimates of the configurational partition functions. The lines are drawn as connected line segments to emphasize the discrete nature of the calculations.

The estimate of α_R followed the procedure suggested by Yamakawa and Stockmayer (see eq 128 of ref 39) that stiff-chain behavior be approximated at arbitrary α_R by use of a closed expression of the Flory form[41]

$$\alpha_R^5 - \alpha_R^3 = K(L/A_K)z \quad (41)$$

Values of α_S, the expansion factor for the radius of gyration, were estimated[10] at several molecular weights from the limiting viscosity number $[\eta]$ in 0.2 M NaCl with use of the Kurata–Yamakawa expression:[42] $\alpha_S = \alpha_\eta^{3/2.43}$, with $\alpha_\eta^3 \equiv [\eta]/[\eta]_0$, where $[\eta]_0$ is the value of $[\eta]$ in the unperturbed state (Θ-solvent). Values of $K(L/A_K)$ were computed from eq 83 of Yamakawa and Stockmayer in order to obtain from eq 41 estimated values of z, which showed the expected dependence on $L^{1/2}$ of eq 40, where $L = 1.0Z$ nm. Here, α_R and α_S were regarded as identical. A similar procedure was used to provide α_R values for a single hyaluronate sample for which $[\eta]$ was measured[43] at several values of I. At each I, a value of z was obtained from eq 41, the constant B was calculated from eq 40, which could then be used to obtain z as a function of L. Values of α_R calculated from eq 41 were then used to correct r_p in eq 38. Correction values of α_R as large as 1.65 were estimated in this way for $I = 0.001$ at $p = 40$, at which point the value of ΔpK was within 1% of convergence.

In Figure 2 the solid lines represent the values of $\Delta pK/\alpha$ calculated from eq 38 at several ionic strengths $I = C_3^*$ as a function of the number p of nearest neighbors included. Convergence was achieved at all ionic strengths by including sufficiently many neighbors.

The summation in eq 38 carried out in this section has involved a single preaveraged value of r_p for each p, chosen as the expansion-corrected unperturbed dimension given by the conformation model used in this work. The model used is therefore equivalent to a rigid structure, which can be termed a "frozen worm" model. This unorthodox summing procedure will clearly give a quite different result from, for example, the assumption of a Gaussian distribution for a chain with fixed ends, which was employed by Katchalsky and Lifson[44] to carry out a similar summation for a continuous, uniform-charge distribution. The justification of use of this ad hoc model is considered in the following section.

Monte Carlo Calculations. A more fundamental approach to the problem involves numerical estimation of the conformational free energy $A_c(Z)$. Such estimates have been carried out by the Monte Carlo method described above for samples of 1000 chains at each Z between 2 and 16 and 500 chains at $Z = 21$ and 26, as well as 100 chains at $Z = 51$. The calculation becomes increasingly inefficient as Z increases because a decreasing fraction of low-energy chains is generated at increasing expenditure of computing time per chain.

Comparison of eq 32 and 35 permits identification of $\langle E_{el} \rangle$ with $\alpha^2 A_c(Z)$; $\langle E_{el} \rangle$ consequently contains the average electrostatic energy as well as the contributions of the configurational entropy contained in $A_c(Z)$. Convergence of $A_c(Z)/Z$ does not occur for the small Z values studied. Convergence can be obtained, however, by noting that subtraction of $A_c(Z)$ from $A_c(Z + 1)$ (eq 35) leads to the more rapidly converging sum of eq 33

$$A_c(Z + 1) - A_c(Z) = (u_1 + u_2 + \ldots + u_Z) = -kT \ln \left(\frac{Q_{Z+1}}{Q_Z Q_{10}} \right) \quad (42)$$

Equation 42, which essentially represents a differentiation of $A_c(Z)$ with respect to Z, requires good precision in the computation to provide acceptable accuracy of the sum in eq 42. Statistical considerations lead to the conclusion that computed mean values of $A_c(Z)$ lie within about 0.25% of the true mean at $Z = 16$ and about 0.5% at $Z = 26$. The accuracy of the differences in eq 42 can be improved by plotting $A_c(Z)$ as a function of Z and graphically smoothing the statistical variation in the individual points. The results are shown in the form $\Delta pK/\alpha = 2\sum u_i/2.3kT$ as the broken lines in Figure 2. Convergence of the sum is obtained for $I \geq 0.005$, but the range of Z is too small to obtain the convergent asymptote at smaller I.

Simultaneous calculation of the ensemble-average electrostatic energy $E_c(Z)$ by averaging at each Z the total electrostatic energy E_{el} with the weighting factor $\exp(-E_{el}/kT)$ and treating the results as for $A_c(Z)$ permits an estimate of the contribution $E_c(\infty)$ to the convergent values $A_c(\infty)$ of $A_c(Z)$. The difference $A_c(\infty) - E_c(\infty)$, which approximates the entropic contribution $-TS(\infty)$ to $A_c(\infty)$, is about 5% of $A_c(\infty)$ at $I = 0.1$, about 7% at $I = 0.01$, and presumably about 10% at $I = 0.001$.

The solid line in Figure 3 presents the convergent values, including extrapolated estimates at $I < 0.005$, of $\Delta pK/\alpha$ from the statistical model as a function of C_3*. Also shown there for purposes of comparison are experimental data for hyaluronic acid titrations[2,3] along with the fits of various uniformly charged cylinder or line charge models.[3]

Discussion

Comparison of Models. As seen in Figure 2, the values of $\Delta pK/\alpha$ obtained as a function of p from the statistical model are surprisingly similar to those from the frozen worm model. The degree of agreement is somewhat fortuitous, as becomes clear when the statistical model is examined in more detail.

When $(R_e)_p$, the distance between the charge sites at $Z = 1$ and $Z = p + 1$, is averaged in the Monte Carlo calculation, expansion due to ionization is found to occur at all values of Z. The expansion factor α_R^2 defined in eq 39 increases with increasing Z and with decreasing I, with values generally larger than those estimated by the Yamakawa–Stockmayer treatment, especially at L near to or less than A_K. This behavior is in qualitative agreement with the treatments of polyion expansion of the continuous wormlike chain,[45,46] which predict increase of the Kuhn length with decreasing ionic strength.

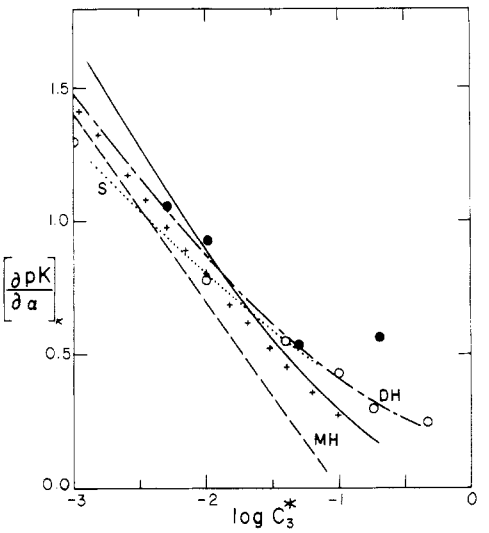

Figure 3. Theoretical slopes of the titration curve of hyaluronic acid are shown as a function of log C_3* for the illustrative example of this work in the convergent ($p = \infty$) extended Bragg–Williams approximation (EBW) from the Monte Carlo calculations. Convergent values were estimated by extrapolation for C_3* < 0.005 M. The crosses indicate the result for the EBW approximation to the linear model with equally spaced sites (eq 46, $b = 1.0$ nm). Other theoretical curves which represent various uniformly charged cylinder models ($\xi = 0.7$) include the Manning–Holtzer (MH) infinite line charge model and the uniformly charged infinite cylinder model for the linearized[6] (DH) and nonlinearized[7] (S) form of the Poisson–Boltzmann equation; all cylinder models have radius $a = 1.0$ nm. The points represent experimental data at various C_3*; symbols as for Figure 1.

The effect of the distribution of site distances on the Coulombic energy and inclusion of entropy terms in A_c in the statistical model just happen to lead to effective values of r_p which approximate those given by the assumptions used with the rigid model. The latter was presented here to suggest that reasonable estimates of the electrostatic energy of stiff-chain molecules can be made by use of such simple models, which resemble conceptually the linear models familiar in polyelectrolyte theory.

Another consequence of the expansion at all p is that the u_p will depend to some extent on the sequence of ionized and nonionized states in the chain for $p > 1$. While a quantitative study has not been made, inclusion of this refinement would introduce a tendency to a higher slope $(\partial pK/\partial\alpha)$ at low α and thus a slightly more negative curvature in the theoretical plots of Figure 1 for both the Ising and EBW models.

Estimates of Error. A. Entropy of Mixing. The use of the EBW approximation to obtain the results shown in Figures 2 and 3 requires some comment. While the ΔpK values from the third-neighbor EBW approximation (and presumably those of higher neighbor approximations) shown in Figure 1 compare favorably with those obtained from the Ising model in the region of α accessible to experiment (α from ca. 0.3 to 0.9), the average slopes of the two plots agree less well. This results from the slightly sigmoidal character of the Ising model result, which leads to an average slope in the experimental region several percent higher than the EBW slope: from 4 to 6% higher at $I = 0.01$ (Table I) and from 5 to 8% higher at $I = 0.001$. The slopes shown in Figure 2 are therefore somewhat smaller than the Ising model values, although this may be compensated somewhat when the dependence of the free energies u_p on sequence of states is introduced.

With this comment in mind, comparison of the results of the present treatment in Figure 3 with the experimental

data indicates that the theory predicts too high values of $\partial pK/\partial\alpha$ at low C_3* and too low values at C_3* greater than about 0.04 M. There are, however, two important factors, and undoubtedly a host of less important ones, which have been neglected in these calculations. The former are taken up in the next section.

B. Effect of Dielectric Constant and Salt Exclusion. Skolnick and Fixman[47] solved the DH equation for the interaction potential of two charges located on the surface of a cylinder of dielectric constant $D_0 = 2$. Their results, presented as a ratio R of the calculated potential to that of the simple screened Coulomb potential used in this work, showed a dependence on both z'/a and ϕ, where z' is the projection on the cylinder axis of the vector between the charges, a is the cylinder radius, and ϕ is the angular displacement of the charge positions around the cylinder cross section. Qualitatively, R increases above unity at small ϕ at any z'/a and decreases below unity at $\phi = 180°$, the magnitude of both effects being largest at small z'/a and large κa.

Since hyaluronic acid is more accurately represented as a wormlike chain[10] than as a rigid cylinder, the Skolnick–Fixman (SF) result is somewhat awkward to introduce into the quantitative computational procedure of this work. A crude estimate of the effect can nevertheless be made, most readily for a somewhat different example than the conformational model used above. Winter et al.[14] reported the crystal structure of a threefold sodium hyaluronate helix which had similar hydrogen-bonding character and charge spacing to the illustrative example used here. The molecular structure had a repeat spacing along the helix axis of 0.95 nm and a (left handed) twist of −120° per disaccharide unit. Although the geometry is helical rather than cylindrical, a calculation ignoring this distinction is possible.

Tables of values of R as a function of ϕ and z'/a were calculated from the results of Skolnick and Fixman. The screened Coulomb potentials appropriate to the approximately linear charge spacing, $r_p = 0.95p$ (nm), were corrected for assumed values of the cylinder radius a between 0.2 nm, which is the charge site radius from the helix axis,[14] and 0.4 nm. The resulting corrections to $\Delta pK/\alpha$, estimated for $a = 0.32$ nm (the unhydrated radius of an assumed cylindrical molecular model; see Introduction) were about −0.10 pK unit at $I = 0.1$ and −0.15 pK unit at $I = 0.01$ and 0.001. Slightly larger corrections (0.02–0.03 pK unit more negative at $I = 0.1$ and up to 0.05 pK unit more negative at $I = 0.001$) were estimated at $a = 0.4$ nm and more positive corrections by about the same amounts at $a = 0.2$ nm. Corresponding estimates for a twofold helix of the same repeat distance ($\phi = 180°$ for nearest-neighbor sites) gave corrections larger in magnitude by about 0.02–0.03 pK unit than the threefold helix.

In solution, of course, hyaluronate does not retain the helical structure. However, examination of the geometry of the low-energy conformations indicates that the nearest-neighbor charged sites do tend to lie on alternate sides of a quasi-helix with an effective average ϕ between −120° and −180°. The corrections quoted may therefore be regarded as reasonable estimates for the solution case, as well. The effect of a correction of −0.15 pK unit on the EBW ($p = \infty$) approximation to the theoretical titration curve is shown as the dotted line in Figure 1. Corrections for this effect would lower the theoretical curve of Figure 3 throughout. At the lowest ionic strengths this effect would correct the curve shown to approximate that of the uniformly charged cylinder ($a = 1.0$ nm) result in the DH approximation. One might reasonably assume that the relative effect seen in Figure 3 for the uniformly charged cylinder (i.e., a further lowering of the curve at low I; compare curves DH and S) would result from solution of the full PB equation for the wormlike chain. The present model thus compares favorably at low ionic strength with the uniformly charged cylinder model without the use of the adjustable cylinder radius of the latter.

C. Counterion Size. The substantial negative deviations at higher ionic strengths are increased by the SF corrections. One explanation for such deviations is the failure of the point-charge potential used to allow correctly for the effects of finite ion size. Approximate corrections for this effect were made in the original Debye–Hückel theory and in the Hill solution for the DH equation for the uniformly charged cylinder by including a charge-free region between the charges of the central ion (or cylinder) and the space charge of the added electrolyte. The effect is always to increase the magnitude of the potential at the charged sites and hence the free energy of interaction of the fixed charges on the cylinder. The magnitude of the correction to ψ_j for two mobile ions and thus to ΔpK based on the simple screened Coulomb potential would be a factor $\exp(\kappa\rho)/(1 + \rho)$, which increases with κ but amounts only to 1.07 at $I = 0.1$ for an ionic radius ρ of 0.4 nm. The correction factor to ΔpK may be larger in the case of the uniformly charged cylinder[6] but is nearly independent of I. A similar result was found by Bailey[48] with assumption of such a charge-free region for a model consisting of periodic discrete charged sites on a dielectric cylinder. A solution of the SF type with this boundary condition would be of interest in this respect. Other effects, including uncertainty about the validity of the PB equation as applied here (electrostatic potentials only), may also affect the results at higher ionic strengths, as they do in solutions of small ions, so that a more sophisticated treatment of the problem is required.

Titration Curve Shape. As shown in Figure 1, the shape of the titration curve predicted by the Ising model is so nearly linear in the region of α accessible to experiment that experimental deviation from linearity would be difficult to detect. In fact, the experimental titration curves appear to be linear when excess salt is present.[3] The effect of the sigmoidal shape would be rather to cause a slightly low estimate of pK_0 upon linear extrapolation of experimental plots of pK_a to $\alpha = 0$. In any case, the full PB solution would be likely to affect the shape of the titration curve, as it does in the case of the uniformly charged cylinder, where a linear result for the DH equation is changed to slight negative curvature throughout by the PB solution, especially at low ionic strength (see Figure 3 of ref 3).

The curve marked M in Figure 1 represents the titration curve for hyaluronic acid calculated from the discrete-site model of Manning,[49] which resembles that of this work in that the simple screened Coulomb potential of eq 8 was used for the site–site interaction energy and that ΔpK was treated in a fashion essentially equivalent to eq 31 with the assumption of random entropy of mixing, so that the entropy term in that equation is zero. In view of this resemblance in approach, it is of interest to inquire into the reason for the substantial difference in the predicted results.

Linear Model. Examination of Manning's expression for the interaction free energy[50] reveals that the result for the fully ionized case is

$$G_{el}/ZkT = -\xi \ln [1 - \exp(-\kappa b)] \qquad (43)$$

where b represents the spacing between the fixed ionized sites in the linear model used and G_{el} can be taken to be

$\langle E_{el} \rangle$ of eq 32. This result is also obtained by substitution of the screened Coulomb potentials u_p used in eq 38 into eq 32 for $\alpha = 1$ and large Z with use of the relation $\ln (1 - x) = -\sum_{t=1}^{\infty}(x^t/t)$, when $x = \exp(-\kappa b)$ and $r_p = tb$. In writing G_{el} for the case of partial ionization, Manning[49] retained the assumption of uniform spacing, so that b is replaced by b/α both in the exponential and in ξ; in addition, the number of charged sites Z becomes $Z\alpha$, so that eq 43 becomes

$$G_{el}/ZkT = -\alpha^2\xi[1 - \exp(-\kappa b/\alpha)] \quad (44)$$

A similar expression appeared in the electrostatic free energy of site interaction within a single statistical chain element in the theory of Rice and Harris,[11b] when equal spacing of charges was assumed as a "crude" model for the element. The present treatment would give for the linear model with equal *ionizable site* spacing b in the EBW approximation (see eq 32)

$$\langle E_{el} \rangle/ZkT = -\alpha^2\xi \ln [1 - \exp(-\kappa b)] \quad (45)$$

Equation 45 differs from eq 44 only in the omission of the factor α in the exponential.

The assumption of a uniform charge spacing at all α leads to the form of eq 44. While consistent with the concept of the continuous line charge model, this assumption is curiously unrealistic in terms of what occurs with change of α in actual polyelectrolyte molecules. In the latter the uniform linear spacing is indeed approximated by the location of the *ionizable sites*, which are fixed in place by the chain structure. The adjustment in position of the sites as the ionization proceeds, which is required by uniform spacing, has no counterpart in the molecule. This is particularly apparent when one considers the polyion at $\alpha = 0.5$, where uniform spacing places the charges reasonably on alternate ionizable sites. As ionization continues, however, the uniform spacing *gradually* moves the charges toward the ultimate nearest-neighbor spacing at $\alpha = 1$. In an actual molecule in which alternate-site ionization (the distribution of lowest energy) is assumed, further charges must appear discretely at points halfway between the already ionized sites, giving rise to a different energy situation, which is illustrated by the difference between eq 44 and 45. The present treatment leading to eq 45 avoids the assumption of uniform spacing by use of the Ising model, which preserves the actual site spacing.

Differentiation of eq 45 and substitution into eq 31 with the entropy term set to zero leads for the linear model with equal site spacing b to

$$\Delta pK/\alpha = -(2\xi/2.3) \ln [1 - \exp(-\kappa b)] \quad (46)$$

while differentiation of eq 44 leads to Manning's result for $\xi < 1$ (eq 63 of ref 49). Equation 46 with $b = 1.0$ nm and $\xi = 0.71$ for hyaluronate produces the points shown as crosses in Figure 3, which would give a curve very similar at $C_3^* < 0.04$ M to the numerical results obtained by making the SF corrections to the theoretical curve shown there (solid line). The decrease in potential due to the larger spacings r_p in the linear model than the conformation model is approximately compensated in eq 46 by neglect of the SF corrections. For $C_3^* > 0.04$ M, the result of eq 46 resembles that of eq 33 (with eq 42) or eq 38.

Equation 46 therefore would appear to be a useful approximation to the more detailed summing required by eq 38 or the extensive calculations required by eq 42. It is of interest to compare eq 46 as an approximate fit to the data to the result plotted in Figure 3 for the model of the uniformly charged cylinder of radius a (DH solution with neglect of the counterion term)[3,6]

$$\Delta pK/\alpha = (2\xi/2.3)[K_0(\kappa a)/\kappa a K_1(\kappa a)] \quad (47)$$

where $K_0(\kappa a)$ and $K_1(\kappa a)$ are modified Bessel functions of the second kind. The function $-\ln [1 - \exp(-\kappa b)]$ resembles closely $K_0(\kappa b)$, even for κb as large as 0.5. At low κa the term in brackets in eq 47 approaches $K_0(\kappa a)$. The good fit to the hyaluronate data by eq 47 with $a = 1.0$ nm can now be understood in the light of the discrete-site model, for which the value $b = 1.0$ nm is the best value for the charge spacing. The identification of a with a "radius" of the polyion modeled as a cylinder, which appeared unreasonably large to us in our discussion of the experimental data in terms of this model,[3] is, in the context of the discrete-site model, not a meaningful concept; the good fit to the experimental data of eq 47 at higher I is presumably fortuitous.

Conclusion

With due allowance for the approximations involved, the results of the present conformational treatment followed by the SF (and presumable PB) corrections give a reasonable fit to the experimental data at low C_3^*. The discrete-site model is a more satisfactory physical representation of the polyion than those used heretofore to interpret the data.[3] It is important to emphasize that no adjustable parameters have been used, other than the choice of the conformation model, which was here required to mimic the unperturbed dimensions and their temperature coefficient rather than to fit the titration data. Equation 46 provides a simple approximation to the corrected version of the result obtained from the conformation model.

Acknowledgment. The author wishes to express on this occasion his feeling of gratitude and indebtedness to his long-time friend and colleague, W. H. Stockmayer, whose assistance and advice at many critical junctures of his career cannot be adequately acknowledged.

Registry No. Hyaluronic acid, 9004-61-9.

References and Notes

(1) Manning, G. S. *J. Chem. Phys.* **1969**, *51*, 924.
(2) Laurent, T. C. Doctoral Thesis, Almqvist and Wiksell, Uppsala, Sweden, 1957.
(3) Cleland, R. L., Wang, J. L.; Detweiler, D. M. *Macromolecules* **1982**, *15*, 386.
(4) Cleland, R. L. *Biopolymers* **1979**, *18*, 2673.
(5) Gorin, M. H. In "Electrophoresis of Proteins"; Abrahamson, H. A., Moyer, L. S., Gorin, M. H., Eds.; Reinhold: New York, 1942; p 126.
(6) Hill, T. L. *Arch. Biochem. Biophys.* **1955**, *57*, 229.
(7) Stigter, D. *J. Colloid Interface Sci.* **1975**, *53*, 296.
(8) Cleland, R. L. *Macromolecules* **1982**, *15*, 382.
(9) Cleland, R. L. *Arch. Biochem. Biophys.* **1977**, *180*, 59.
(10) Cleland, R. L. *Biopolymers*, in press.
(11) (a) Harris, F. E.; Rice, S. A. *J. Phys. Chem.* **1954**, *58*, 725. (b) Rice, S. A.; Harris, F. E. *Ibid.* **1954**, *58*, 733.
(12) Cleland, R. L. *Biopolymers* **1971**, *10*, 1925.
(13) Arnott, S.; Scott, W. E. *J. Chem. Soc., Perkin Trans. 2* **1972**, 324.
(14) Winter, W. T.; Smith, P. J. C.; Arnott, S. *J. Mol. Biol.* **1975**, *99*, 219.
(15) Cleland, R. L. *Biopolymers* **1979**, *18*, 1821.
(16) Cleland, R. L. These unpublished results were presented in part at the Symposium on Solution Properties of Polysaccharides, 179th National Meeting of the American Chemical Society, Houston, Texas, in Mar 1980.
(17) Abe, A. *J. Am. Chem. Soc.* **1976**, *98*, 6477.
(18) Jeffrey, G. A.; Pople, J. A.; Binkley, J. S.; Vishveshwara, S. J. *J. Am. Chem. Soc.* **1978**, *100*, 373.
(19) Brant, D. A.; Goebel, K. D. *Marcromolecules* **1972**, *5*, 536.
(20) Mathews, M. B.; Decker, L. *Biochim. Biophys. Acta* **1977**, *498*, 259.
(21) Momany, F. A.; Carruthers, L. M.; McGuire, R. F.; Scheraga, H. A. *J. Phys. Chem.* **1974**, *78*, 1595.
(22) Hasted, J. B.; Ritson, D. M.; Collie, C. H. *J. Chem. Phys.* **1948**, *16*, 1.
(23) Fixman, M. *J. Chem. Phys.* **1979**, *70*, 4995.

(24) Rice, S. A.; Nagasawa, M. "Polyelectrolyte Solutions"; Academic Press: New York, 1961; Chapter 7.
(25) Hill, T. L. *Faraday Discuss. Chem. Soc.* **1956**, *21*, 31. Stigter, D.; Hill, T. L. *J. Phys. Chem.* **1959**, *63*, 551.
(26) Schildkraut, C.; Lifson, S. *Biopolymers* **1965**, *3*, 195.
(27) Guss, J. M.; Hukins, W. L.; Smith, P. J. C.; Winter, W. T.; Arnott, S. *J. Mol. Biol.* **1975**, *95*, 359.
(28) Ising, E. *Z. Phys.* **1925**, *31*, 253.
(29) Schwarz, G. *Biopolymers* **1968**, *6*, 873.
(30) Schwarz, G. *Eur. J. Biochem.* **1970**, *12*, 442.
(31) Hill, T. L. *J. Am. Chem. Soc.* **1956**, *78*, 5527.
(32) Sasaki, S.; Minakata, A. *Biophys. Chem.* **1980**, *11*, 199.
(33) Kramers, H. A.; Wannier, G. H. *Phys. Rev.* **1941**, *60*, 252.
(34) Flory, P. J. "Statistical Mechanics of Chain Molecules"; Interscience: New York, 1969; Chapter 3.
(35) Marchi, E.; Vila, J. *J. Phys. A.: Math. Gen.* **1980**, *13*, 2465.
(36) Rutledge, G. *Phys. Rev.* **1932**, *40*, 262.
(37) Bragg, W. L.; Williams, E. J. *Proc. R. Soc. London* **1934**, *145*, 699.
(38) Overbeek, J. T. G. *Bull. Soc. Chim. Belg.* **1948**, *57*, 252.
(39) Yamakawa, H.; Stockmayer, W. H. *J. Chem. Phys.* **1972**, *57*, 2843.
(40) Orofino, T. A.; Flory, P. J. *J. Chem. Phys.* **1957**, *26*, 1067.
(41) Flory, P. J. *J. Chem. Phys.* **1949**, *17*, 303.
(42) Kurata, M.; Yamakawa, H. *J. Chem. Phys.* **1958**, *29*, 311.
(43) Cleland, R. L. *Biopolymers* **1968**, *6*, 1519.
(44) Katchalsky, A.; Lifson, S. *J. Polym. Sci.* **1953**, *11*, 409.
(45) Odijk, T. *J. Polym. Sci.* **1977**, *15*, 477.
(46) Skolnick, J.; Fixman, M. *Macromolecules* **1977**, *10*, 944.
(47) Skolnick, J.; Fixman, M. *Macromolecules* **1978**, *11*, 867.
(48) Bailey, J. M. *Biopolymers* **1973**, *12*, 559.
(49) Manning, G. S. *J. Phys. Chem.* **1981**, *85*, 870.
(50) Manning, G. S. *Acc. Chem. Res.* **1971**, *12*, 443. In the present work the distinction between G_{el}, the Gibbs free energy, and A_{el}, the Helmholtz free energy of charging the system has been ignored. The distinction is concerned with whether the charging process is carried out at constant temperature and pressure (G_{el}) or constant temperature and volume (A_{el}).

Effect of Loop Entropy on the Helix–Coil Transition of α-Helical, Two-Chain, Coiled Coils. 3. Supermatrix Formulation of the Imperfect-Matching Model†

Jeffrey Skolnick

Department of Chemistry, Washington University, St. Louis, Missouri 63130.
Received April 28, 1983

ABSTRACT: The theory of the α-helix-to-random coil transition of two-chain, coiled coils (dimers) has been extended to include the possibility of mismatched association of the chains, viz., the loops-excluded, imperfect-matching model. Since loop entropy essentially restricts the number of interacting helical regions in the dimers to one, the only mismatched conformations consistent with this constraint are the out-of-register ones. Serial matrix product expressions for the internal partition function of the dimer, for the overall helix content, for the helix probability profiles, and for the ratio of the number of randomly coiled residues part of the random coil runs from the chain ends to the total number of random coils are derived. The loops-excluded, imperfect-matching model is applied to hypothetical homopolymeric coiled coils, and the qualitative effect of region specificity of the helix–helix interaction parameter on the character of the helix–coil transition is investigated. Comparison is also made between the present model and the loops-excluded, perfect-matching model developed previously, in which only in-register conformations are allowed.

I. Introduction

In a recent series of papers we have developed the theory of the α-helix-to-random coil transition of two-chain, coiled coils in the perfect-matching approximation.[1-4] That is, we a priori assumed that the portions of the two-chain, coiled coil (dimers) that are helical remain in-register throughout the course of the helix-to-random coil transition. Since it is presumably the interhelical interaction between chains that is responsible for the greatly enhanced helix content of the dimer relative to the isolated single chains, in the limit of 100% helix, the perfect-matching approximation is valid. However, as the helix content of the dimer decreases, the relative importance of out-of-register associations of the two chains, i.e., mismatch, increases: thus mismatched conformations would be expected to be important in the transition region of the thermal denaturation profile. To date, we have entirely ignored this effect. The purpose of the present paper is to extend the theory of the helix-to-coil transition in two-chain, coiled coils to include, via an extension of the supermatrix formulation developed previously,[4] the possibility of mismatched association of the chains. By way of illustration the theory will be applied to hypothetical dimers composed of identical, homopolymeric single chains but whose interhelical interactions may be region dependent.

At this juncture it is appropriate to review the fundamental assumptions of previous work that are applicable to two-chain, coiled coils with mismatch:[1,3]

(1) To account for the short-range interactions, the theory is formulated in terms of the Zimm–Bragg parameters σ and $s(T)$ characteristic of the individual amino acids in the isolated protein chains.[5] σ and $s(T)$ are assumed to depend only on the type of amino acid and are assumed to be independent of the type of nearest neighbor. Recent experimental verification of this assumption has been provided (at least for the isolated single chains in solution) by Kidera et al. for the case of single-chain, random copolymers of (hydroxypropyl)-L-glutamine, L-alanine, and glycine.[6] The practical realization of the theory for proteins such as tropomyosin requires the knowledge of the primary sequence of the molecule and the table of σ and $s(T)$ values for the various poly(amino acids) determined in a impressive experimental effort by Scheraga et al.;[7-20] these expressions have been summarized recently in a convenient algorithmic form.[21,22]

(2) To account for the long-range interactions believed responsible for the greatly augmented helix content of the

† This paper is dedicated to Professor Walter H. Stockmayer—a scientist and a gentleman in the very best sense of the words.

0024-9297/84/2217-0645$01.50/0